Attitude Tracking Control for a Quadrotor UAV Using an Adaptive Chattering-Free SMC

Mert Serhat Sarıhan
Control & Automation Engineering
Institute Of Graduate Programs
Istanbul Technical University
Istanbul, Turkey
sarihan22@itu.edu.tr

Fatih Adıgüzel
Control & Automation Engineering
Faculty of Electric-Electronic
Yildiz Technical University
Istanbul, Turkey
fadiguzel@yildiz.edu.tr

Fikret Çalışkan
Control & Automation Engineering
Faculty of Electric-Electronic
Istanbul Technical University
Istanbul, Turkey
caliskanf@itu.edu.tr

***Abstract*—This paper addresses an adaptive sliding mode nonlinear controller design for the attitude tracking of an autonomous quadrotor unmanned aerial vehicle (UAV). To overcome the chattering phenomenon in the controller signals, the proposed design is realized by considering the integral of the controller signal. In addition, Lyapunov-based estimations are employed, instead of bounded values of nonlinear functions and their derivatives in the controller design. Thus, the nonlinear functions that impose a computational burden on the controller signal in the classical nonlinear control method are used with their upper bounds estimated in the design. Furthermore, a singularity-free sliding mode approach is proposed to avoid the potential singularities in the adaptation mechanism. The asymptotic stability of the closed-loop dynamics is proved in the sense of Lyapunov theory. The effectiveness of the proposed control method is verified by comparative numerical simulations of the quadrotor UAV, demonstrating the robustness of the controller against external disturbances, model uncertainties, and partial actuator faults.**

***Index Terms*—Sliding mode control, adaptive control, attitude tracking, passive FTC, quadrotor UAV**

I. Introduction

Autonomous quadrotor UAVs are widely used in tasks ranging from search and rescue missions to industrial inspection [1]. Their ability to perform vertical take-off and landing, hovering, and performing agile maneuvers sets them apart from fixed-wing unmanned aerial vehicles. However, these advantages come with inherent challenges. Quadrotor UAVs are underactuated and strongly coupled systems that are subject to modeling uncertainties such as unknown payloads and actuator faults. As a result, developing advanced control schemes that ensure stability, achieve rapid response, and reject disturbances effectively is a complex task.

A variety of linear and nonlinear control methodologies have been researched and reviewed, such as Linear Quadratic Regulator (LQR), Proportional-Integral-Derivative (PID), gain scheduling, H_∞, fault tolerant, model predictive, backstepping, and feedback linearization control methods to stabilize and navigate the quadrotor systems [2]–[7]. In [8]–[11], PID-based control schemes were applied to stabilize and navigate various quadrotor systems. In addition to classical PID-based approaches, nonlinear control techniques have also been widely explored for quadrotor control. For instance, feedback linearization (FL) methods were applied for trajectory tracking in [12], [13]. Similarly, backstepping control techniques have also been utilized for trajectory tracking in quadrotor systems, as presented in [14], [15].

Over the years SMC has drawn significant attention due to its robustness against model uncertainties and external disturbances. In [16]–[20], SMC was used to control the position and attitude of a quadrotor system. Despite their contributions in [18], [19], external disturbances; in [16], model uncertainties, and in [17], [20] actuator faults have not been taken into account. To augment robustness against model uncertainties and external disturbances, adaptive sliding mode control (ASMC) schemes have been developed [12], [21], where ASMC clearly demonstrates superiority over feedback linearization (FL) in [12]. Although chattering reduction is considered in [12], [16]; it is not explicitly addressed in [17]–[19], [21]. To alleviate the chattering phenomenon, diverse Integral Sliding Mode Control (ISMC) techniques have been proposed [22]–[27], yet none of the studies have achieved its complete elimination.

In this study, an adaptive integral sliding mode controller (AISMC) is proposed to address the chattering phenomenon and enhance robustness under model uncertainties and external disturbances in quadrotor systems. Unlike conventional sliding mode control approaches, the differentiation of the control signal is evaluated as the controller signal and then integrated to generate the actual control input. This structure effectively eliminates high-frequency switching behavior, resulting in a chattering-free response. Lyapunov-based adaptation mechanisms are incorporated into the controller design to enhance the robustness of the proposed control scheme under model uncertainties and external disturbances. The adaptation mechanisms eliminate the need for upper bound values of parametric uncertainties and time-varying external disturbances, thereby significantly reducing their impact on the system's performance. Furthermore, an additional adaptation law is introduced

to address the controller gain uncertainty associated with the control signal, enabling the controller to maintain performance in the presence of actuator faults, thus ensuring fault-tolerant control. The proposed AISMC, along with the adaptive laws, is mathematically proven to ensure system stability based on Lyapunov theory.

II. Mathematical Model

The nonlinear dynamical system model is derived using the Newton-Euler method [9], [28], [29]. The quadrotor geometry and related frames are given in Fig. 1. The dynamic model of the quadrotor is formulated using two coordinate frames: the body-fixed frame $\mathcal{B}$ and the inertial frame $\mathcal{E}$. The quadrotor requires six state variables to fully characterize its attitude motion, as illustrated below:

$$\begin{bmatrix} \dot{\phi} \\ \dot{p} \\ \dot{\theta} \\ \dot{q} \\ \dot{\psi} \\ \dot{r} \end{bmatrix} = \begin{bmatrix} p + q\sin\phi\tan\theta + r\cos\phi\tan\theta \\ \frac{J_y - J_z}{J_x} qr + \frac{u_\phi}{J_x} \\ q\cos\phi - r\sin\phi \\ \frac{J_z - J_x}{J_y} pr + \frac{u_\theta}{J_y} \\ q\sin\phi\sec\theta + r\cos\phi\sec\theta \\ \frac{J_x - J_y}{J_z} pq + \frac{u_\psi}{J_z} \end{bmatrix} \tag{1}$$

where the variables ϕ, θ, and ψ represent the roll, pitch, and yaw orientations of the quadrotor with respect to the inertial frame. These angles are bounded as follows: $-\frac{\pi}{2} < \phi < \frac{\pi}{2}$ for roll, $-\frac{\pi}{2} < \theta < \frac{\pi}{2}$ for pitch, and $-\pi < \psi < \pi$ for yaw. The variables p, q, and r correspond to the angular velocities around the body frame's roll, pitch, and yaw axes, respectively. The control inputs u_ϕ, u_θ, and u_ψ represent the net torques acting on the quadrotor. The parameters J_x, J_y, and J_z denote the moments of inertia around the x, y, and z axes. The control inputs can be expressed as

$$\begin{bmatrix} u_\phi \\ u_\theta \\ u_\psi \end{bmatrix} = \begin{bmatrix} -bl/\sqrt{2} & bl/\sqrt{2} & bl/\sqrt{2} & -bl/\sqrt{2} \\ bl/\sqrt{2} & -bl/\sqrt{2} & bl/\sqrt{2} & -bl/\sqrt{2} \\ -d & -d & d & d \end{bmatrix} \begin{bmatrix} \omega_1^2 \\ \omega_2^2 \\ \omega_3^2 \\ \omega_4^2 \end{bmatrix} \tag{2}$$

where ω_i is the angular speed of the i-th rotor, and l is the distance from each rotor to the quadrotor's center of mass. The constants b and d represent the thrust and drag coefficients, respectively. With small-angle approximations, the simplified form of the quadrotor dynamics in (1) is as follows:

$$\begin{bmatrix} \dot{x}_1 \\ \dot{x}_2 \\ \dot{x}_3 \\ \dot{x}_4 \\ \dot{x}_5 \\ \dot{x}_6 \end{bmatrix} = \begin{bmatrix} x_2 \\ \frac{J_y - J_z}{J_x} x_4 x_6 + \frac{u_\phi}{J_x} \\ x_4 \\ \frac{J_z - J_x}{J_y} x_2 x_6 + \frac{u_\theta}{J_y} \\ x_6 \\ \frac{J_x - J_y}{J_z} x_2 x_4 + \frac{u_\psi}{J_z} \end{bmatrix}. \tag{3}$$

III. Controller Design

This section focuses on the design of the attitude control inputs u_ϕ, u_θ, and u_ψ based on integral sliding manifolds. An adaptive law is integrated into the control structure to compensate for system uncertainties and disturbances, and the closed-loop stability is analytically ensured through Lyapunov theory. Instead of developing controllers for each attitude channel individually, only the roll control input is derived in detail for simplicity. The final control laws for the pitch and yaw channels are presented later without intermediate derivations.

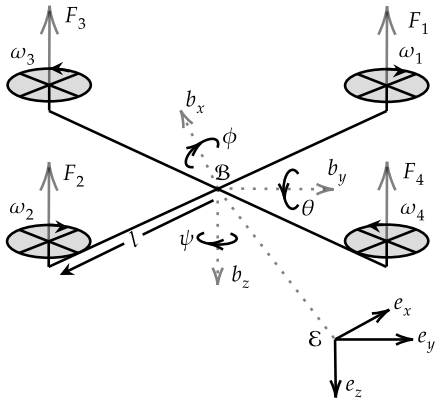

Fig. 1. Quadrotor geometry.

The roll channel dynamics in (3) are reformulated using the newly introduced notation as

$$\begin{cases} \dot{x}_1 = x_2 \\ J_x \dot{x}_2 = (J_y - J_z) x_4 x_6 + u_\phi + d_\phi \end{cases} \tag{4}$$

where d_ϕ represents the external disturbance on the roll dynamics. As shown in (5), the control input u_ϕ appears in an additive form without any multiplicative factor, which enables the dynamics to be cast into an affine structure: $\Theta_{\phi_0} \dot{x}_2 = f_\phi + \Delta f_\phi + u_\phi$. Here, Θ_{ϕ_0} denotes a partially known parameter subject to modeling uncertainty, while Δf_ϕ represents a lumped term capturing both model uncertainties and external disturbances. The errors are defined as

$$\begin{cases} e_\phi = \phi_d - x_1 \\ \dot{e}_\phi = \dot{\phi}_d - x_2 \end{cases} \tag{5}$$

where ϕ_d and $\dot{\phi}_d$ represent the desired roll angle and its time derivative, respectively. The sliding surface is designed as

$$s_\phi = \dot{e}_\phi + \lambda_{1\phi} \int_0^t \dot{e}_\phi \, d\tau + \lambda_{2\phi} \int_0^t e_\phi \, d\tau \tag{6}$$

where $\lambda_{1\phi}$ and $\lambda_{2\phi}$ are design parameters. When the quadrotor is at an equilibrium point, the sliding surface is expected to reach zero, thereby yielding the solution of (6) as

$$\begin{bmatrix} \dot{e}_\phi \\ \ddot{e}_\phi \end{bmatrix} = \begin{bmatrix} 0 & 1 \\ -\lambda_{2\phi} & -\lambda_{1\phi} \end{bmatrix} \begin{bmatrix} e_\phi \\ \dot{e}_\phi \end{bmatrix} \tag{7}$$

where the parameters $\lambda_{1\phi}$ and $\lambda_{2\phi}$ are to be selected such that the characteristic polynomial of (7) is Hurwitz stable. Using the sliding surface (6), a sliding manifold is designed as

$$\sigma_\phi = \dot{s}_\phi + c_\phi s_\phi \tag{8}$$

where c_ϕ is a positive design parameter, i.e., $c_\phi > 0$. The time derivative of (8) is

$$\begin{aligned}\dot{\sigma}_\phi &= \ddot{s}_\phi + c_\phi \dot{s}_\phi \\ &= \dddot{e}_\phi + \lambda_1 \ddot{e}_\phi + \lambda_2 \dot{e}_\phi + c_\phi(\ddot{e}_\phi + \lambda_1 \dot{e}_\phi + \lambda_2 e_\phi).\end{aligned} \tag{9}$$

A positive definite candidate Lyapunov function is given as

$$V_\phi(t) = \frac{1}{2}\Theta_{\phi_0}\sigma_\phi^2 + \sum_{i=0}^{4} \frac{1}{2\gamma_{\phi_i}} \tilde{\Theta}_{\phi_i}^2 \tag{10}$$

where $\tilde{\Theta}_{\phi_i} = \hat{\Theta}_{\phi_i} - \Theta_{\phi_i}$. The first-order derivative of the Lyapunov candidate function (10) is

$$\begin{aligned}\dot{V}_\phi(t) &= \Theta_{\phi_0}\sigma_\phi\dot{\sigma}_\phi + \sum_{i=0}^{4} \frac{1}{\gamma_{\phi_i}} \dot{\hat{\Theta}}_{\phi_i}\tilde{\Theta}_{\phi_i} \\ &= \Theta_{\phi_0}\sigma_\phi(\ddot{s}_\phi + c_\phi \dot{s}_\phi) + \sum_{i=0}^{4} \frac{1}{\gamma_{\phi_i}} \dot{\hat{\Theta}}_{\phi_i}\tilde{\Theta}_{\phi_i}.\end{aligned} \tag{11}$$

The expanded form of (11) is

$$\begin{aligned}\dot{V}_\phi(t) = \Theta_{\phi_0}\sigma_\phi\Big(&\dddot{e}_\phi + \lambda_{1\phi}\ddot{e}_\phi + \lambda_{2\phi}\dot{e}_\phi \\ &+ c_\phi\big(\ddot{e}_\phi + \lambda_{1\phi}\dot{e}_\phi + \lambda_{2\phi}e_\phi\big)\Big) + \sum_{i=0}^{4} \frac{1}{\gamma_{\phi_i}} \dot{\hat{\Theta}}_{\phi_i}\tilde{\Theta}_{\phi_i}.\end{aligned} \tag{12}$$

Re-writing (12) in terms of $\Theta_{\phi_0}\dot{x}_2 = f_\phi + \Delta f_\phi + u_\phi$ notation, (12) turns into as follows:

$$\begin{aligned}\dot{V}_\phi(t) = \sigma_\phi\Big(&\dot{f}_\phi + \Delta\dot{f}_\phi + \dot{u}_\phi + (\lambda_{1\phi} + c_\phi)(f_\phi + \Delta f_\phi + u_\phi) \\ &- \Theta_{\phi_0}\beta_\phi\Big) + \sum_{i=0}^{4} \frac{1}{\gamma_{\phi_i}} \dot{\hat{\Theta}}_{\phi_i}\tilde{\Theta}_{\phi_i}\end{aligned} \tag{13}$$

where $\beta_\phi = \dddot{\phi}_d + \lambda_{1\phi}\ddot{\phi}_d - \lambda_{2\phi}\dot{\phi}_d + c_\phi(\ddot{\phi}_d - \lambda_{1\phi}\dot{e}_\phi - \lambda_{2\phi}e_\phi)$. Let's define the bounded unknown values $(\Theta_{\phi_1}, \Theta_{\phi_2}, \Theta_{\phi_3}, \Theta_{\phi_4})$ related to $\dot{f}_\phi$, $\Delta\dot{f}_\phi$, f_ϕ and Δf_ϕ:

$$\begin{aligned}\dot{V}_\phi(t) \le \sigma_\phi\Big(&\Theta_{\phi_1} + \Theta_{\phi_2} + \dot{u}_\phi + (\lambda_{1\phi} + c_\phi)(\Theta_{\phi_3} + \Theta_{\phi_4} + u_\phi) \\ &- \Theta_{\phi_0}\beta_\phi\Big) + \sum_{i=0}^{4} \frac{1}{\gamma_{\phi_i}} \dot{\hat{\Theta}}_{\phi_i}\tilde{\Theta}_{\phi_i}.\end{aligned} \tag{14}$$

If $\dot{u}_\phi$ is defined as

$$\begin{aligned}\dot{u}_\phi(t) = -\text{sign}(\sigma_\phi)\Big(&\hat{\Theta}_{\phi_1} + \hat{\Theta}_{\phi_2} + (\lambda_{1\phi} + c_\phi)\big(\hat{\Theta}_{\phi_3} + \hat{\Theta}_{\phi_4}\big) \\ &- \hat{\Theta}_{\phi_0}\beta_\phi\Big) - (\lambda_{1\phi} + c_\phi)u_\phi - K_\phi|\sigma_\phi|\end{aligned} \tag{15}$$

then $\dot{V}_\phi(t)$ becomes

$$\begin{aligned}\dot{V}_\phi(t) \le\ &\tilde{\Theta}_{\phi_0}\Big(\frac{1}{\gamma_{\phi_0}}\dot{\hat{\Theta}}_{\phi_0} + \beta_\phi|\sigma_\phi|\Big) + \tilde{\Theta}_{\phi_1}\Big(\frac{1}{\gamma_{\phi_1}}\dot{\hat{\Theta}}_{\phi_1} - |\sigma_\phi|\Big) \\ &+ \tilde{\Theta}_{\phi_2}\Big(\frac{1}{\gamma_{\phi_2}}\dot{\hat{\Theta}}_{\phi_2} - |\sigma_\phi|\Big) + \tilde{\Theta}_{\phi_3}\Big(\frac{1}{\gamma_{\phi_3}}\dot{\hat{\Theta}}_{\phi_3} - (\lambda_{1\phi} + c_\phi)|\sigma_\phi|\Big) \\ &+ \tilde{\Theta}_{\phi_4}\Big(\frac{1}{\gamma_{\phi_4}}\dot{\hat{\Theta}}_{\phi_4} - (\lambda_{1\phi} + c_\phi)|\sigma_\phi|\Big) - K_\phi|\sigma_\phi|.\end{aligned} \tag{16}$$

If the adaptation rules are selected as follows:

$$\begin{aligned}&\dot{\hat{\Theta}}_{\phi_0} = -\gamma_{\phi_0}\beta_\phi|\sigma_\phi|,\ \dot{\hat{\Theta}}_{\phi_1} = \gamma_{\phi_1}|\sigma_\phi|,\ \dot{\hat{\Theta}}_{\phi_2} = \gamma_{\phi_2}|\sigma_\phi|, \\ &\dot{\hat{\Theta}}_{\phi_3} = \gamma_{\phi_3}(\lambda_{1\phi} + c_\phi)|\sigma_\phi|,\ \dot{\hat{\Theta}}_{\phi_4} = \gamma_{\phi_4}(\lambda_{1\phi} + c_\phi)|\sigma_\phi|,\end{aligned} \tag{17}$$

then $\dot{V}_\phi(t)$ becomes

$$\dot{V}_\phi(t) \le -K_\phi|\sigma_\phi| \tag{18}$$

which proves the asymptotic stability according to the LaSalle–Yoshizawa Theorem, as the first-order derivative of the Lyapunov candidate function is negative definite.

The sliding surfaces for the pitch and yaw channels are defined as

$$\begin{aligned}s_\theta &= \dot{e}_\theta + \lambda_{1\theta}\int_0^t \dot{e}_\theta\, d\tau + \lambda_{2\theta}\int_0^t e_\theta\, d\tau \\ s_\psi &= \dot{e}_\psi + \lambda_{1\psi}\int_0^t \dot{e}_\psi\, d\tau + \lambda_{2\psi}\int_0^t e_\psi\, d\tau\end{aligned} \tag{18}$$

where the errors are

$$\begin{aligned}e_\theta &= \theta_d - x_3, \quad \dot{e}_\theta = \dot{\theta}_d - x_4 \\ e_\psi &= \psi_d - x_5, \quad \dot{e}_\psi = \dot{\psi}_d - x_6.\end{aligned} \tag{19}$$

Similarly, if $\dot{u}_\theta(t)$ and $\dot{u}_\psi(t)$ signals for the pitch and yaw channel are designed as

$$\begin{aligned}\dot{u}_\theta(t) = -\text{sign}(\sigma_\theta)\Big(&\hat{\Theta}_{\theta_1} + \hat{\Theta}_{\theta_2} + (\lambda_{1\theta} + c_\theta)\big(\hat{\Theta}_{\theta_3} + \hat{\Theta}_{\theta_4}\big) \\ &- \hat{\Theta}_{\theta_0}\beta_\theta\Big) - (\lambda_{1\theta} + c_\theta)u_\theta - K_\theta|\sigma_\theta|\end{aligned} \tag{20}$$

$$\begin{aligned}\dot{u}_\psi(t) = -\text{sign}(\sigma_\psi)\Big(&\hat{\Theta}_{\psi_1} + \hat{\Theta}_{\psi_2} + (\lambda_{1\psi} + c_\psi)\big(\hat{\Theta}_{\psi_3} + \hat{\Theta}_{\psi_4}\big) \\ &- \hat{\Theta}_{\psi_0}\beta_\psi\Big) - (\lambda_{1\psi} + c_\psi)u_\psi - K_\psi|\sigma_\psi|\end{aligned} \tag{21}$$

with the following adaptation laws

$$\begin{cases}\dot{\hat{\Theta}}_0 = -\gamma_{\theta_0}\beta_\theta|\sigma_\theta|, \\ \dot{\hat{\Theta}}_1 = \gamma_{\theta_0}|\sigma_\theta|, \\ \dot{\hat{\Theta}}_2 = \gamma_{\theta_0}|\sigma_\theta|, \\ \dot{\hat{\Theta}}_3 = \gamma_{\theta_0}(\lambda_{1\theta} + c)|\sigma_\theta|, \\ \dot{\hat{\Theta}}_4 = \gamma_{\theta_0}(\lambda_{1\theta} + c)|\sigma_\theta|\end{cases}, \begin{cases}\dot{\hat{\Theta}}_{\psi_0} = -\gamma_{\psi_0}\beta_\psi|\sigma_\psi|, \\ \dot{\hat{\Theta}}_{\psi_1} = \gamma_{\psi_1}|\sigma_\psi|, \\ \dot{\hat{\Theta}}_{\psi_2} = \gamma_{\psi_2}|\sigma_\psi|, \\ \dot{\hat{\Theta}}_{\psi_3} = \gamma_{\psi_3}(\lambda_{1\psi} + c_\phi)|\sigma_\psi|, \\ \dot{\hat{\Theta}}_{\psi_4} = \gamma_{\psi_4}(\lambda_{1\psi} + c_\phi)|\sigma_\psi|\end{cases} \tag{22}$$

then the resultant first order derivatives of the Lyapunov candidate functions are

$$\dot{V}_\theta(t) \le -K_\theta|\sigma_\theta|, \quad \dot{V}_\psi(t) \le -K_\psi|\sigma_\psi| \tag{23}$$

thereby proving the asymptotic stability according to the LaSalle–Yoshizawa Theorem for pitch and yaw channels.

IV. Simulation Results

This section provides simulation studies conducted to evaluate the performance of the proposed controller in comparison with a conventional PID controller and the SMC controller presented in [17]. The simulations are implemented in MATLAB/Simulink with a fixed-step solver using the fourth-order

TABLE I
QUADROTOR PHYSICAL PARAMETERS

Parameter	Symbol	Value	Unit
Quadcopter mass	m	1.590	kg
Roll inertia	J_x	0.1065	kg·m^2
Pitch inertia	J_y	0.1105	kg·m^2
Yaw inertia	J_z	0.140	kg·m^2
Arm length	l	0.243	m
Thrust coefficient	b	2.02×10^{-7}	N·rpm^{-2}
Drag coefficient	d	4.18×10^{-9}	N·m·rpm^{-2}

TABLE II
RMS VALUES OF CONTROL SIGNALS

Controller	Scenario-1			Scenario-2			Scenario-3		
	u_ϕ	u_θ	u_ψ	u_ϕ	u_θ	u_ψ	u_ϕ	u_θ	u_ψ
PID	.007	.007	.003	.010	.016	.072	.016	.016	.015
SMC	.048	.042	.019	.045	.051	.101	.052	.050	.029
AISMC	.004	.004	.005	.016	.020	.078	.014	.014	.016

Runge-Kutta method and a sampling time of 0.01 seconds. Three different simulation scenarios are considered to show the effectiveness of the proposed controller.

The parameters of the quadrotor are given in Table I. The parameters of the PID controllers are chosen as: $K_{P\phi} = K_{P\theta} = 0.05; K_{P\psi} = 3; K_{I\phi} = K_{I\theta} = K_{I\psi} = 0.01; K_{D\phi} = K_{D\theta} = 0.5; K_{D\psi} = 2$. The parameters of the SMC controller adopted from [17] are selected as: $C_\phi = C_\theta = 0.2; C_\psi = 2; K_{1\phi} = K_{1\theta} = K_{1\psi} = 0.001; K_{2\phi} = K_{2\theta} = K_{2\psi} = 1$. The parameters of the proposed controllers are set to: $\lambda_{1\phi} = \lambda_{1\theta} = \lambda_{1\psi} = 5; \lambda_{2\phi} = \lambda_{2\theta} = \lambda_{2\psi} = 1; c_\phi = c_\theta = c_\psi = 100; \Theta_{\{0,1,2,3,4\}\phi} = \Theta_{\{0,1,2,3,4\}\theta} = \Theta_{\{0,1,2,3,4\}\psi} = 0.0001; K_\phi = K_\theta = K_\psi = 1$.

In the first scenario, with no external disturbances, model uncertainties, or actuator faults are present, the simulation results indicate that the PID, the SMC and the proposed controllers provide similar reference tracking performances as illustrated in Fig. 2. Although the control signals appear similar for the PID and the proposed AISMC controllers in Fig. 3, the SMC exhibits noticeable chattering.

In the second scenario, the quadrotor UAV system is subjected to time-varying disturbances with a non-zero mean, considered as sinusoidal moments of the form $0.005\sin(4t)+0.06$ [N·m] applied to the body frame $\mathcal{B}$, along with a 30% model uncertainty in the inertia, thrust coefficient, and drag coefficient parameters. In this case, despite the similar performances of the SMC and the AISMC in the roll and pitch channels, the SMC exhibits chattering and a greater effort in the control signal compared to the AISMC, as shown in Table II. The PID controller, on the other hand, displays a control effort similar to that of the AISMC, but performs worse in tracking in the roll and pitch channels. In the yaw channel, while the control signals produced by the PID controller and AISMC are similar, the AISMC achieves noticeably improved tracking accuracy, highlighting its robustness, whereas the conventional

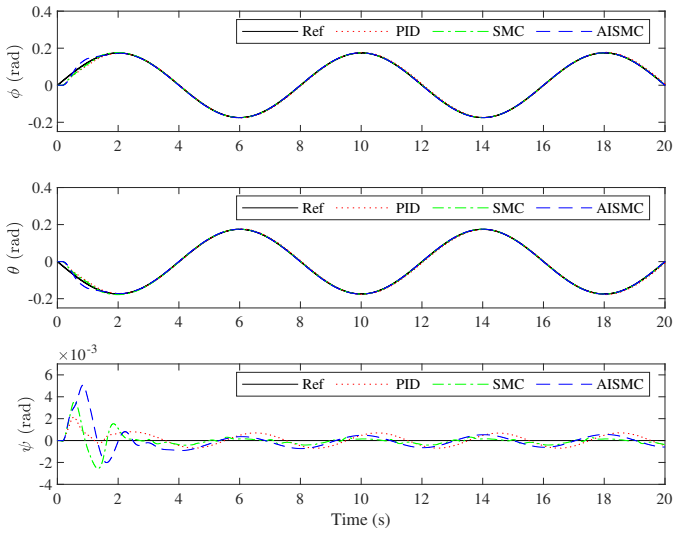

Fig. 2. Attitude responses without disturbances and model uncertainties.

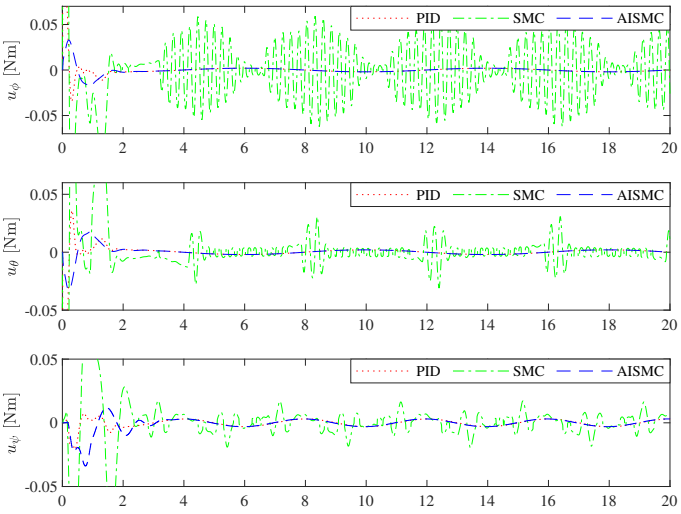

Fig. 3. Control signals without disturbances and model uncertainties.

SMC yields poorer tracking performance with a greater control signal. The results for this scenario are presented in Fig. 4, with the control inputs illustrated in Fig. 5.

In the third scenario, a 10% fault is injected into the first actuator at the 10th second. Although both the PID and the SMC controllers fail to track under this condition, the AISMC successfully compensates for the fault through its inherent passive fault-tolerant capability. The simulation results for this case are given in Fig. 6, and the associated control signals are shown in Fig. 7. In scenario three, the uncertain control

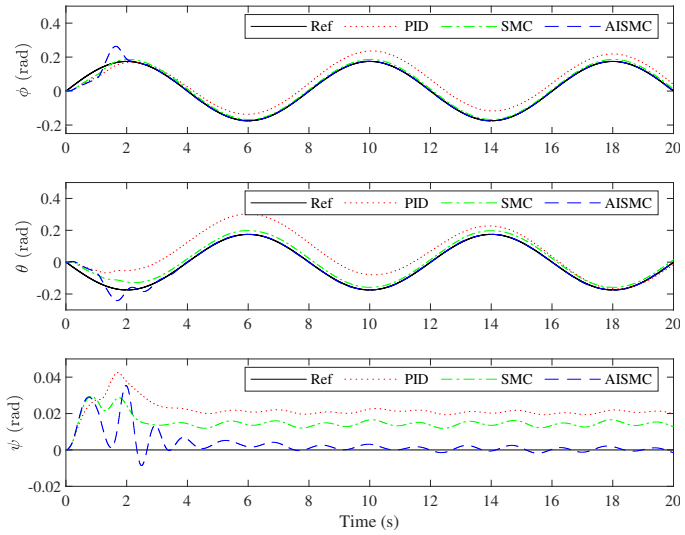

Fig. 4. Attitude responses under disturbances and model uncertainties.

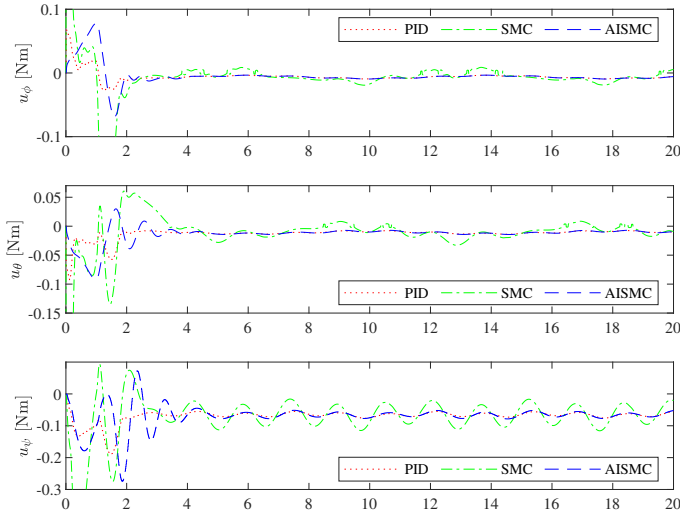

Fig. 5. Control signals under disturbances and model uncertainties.

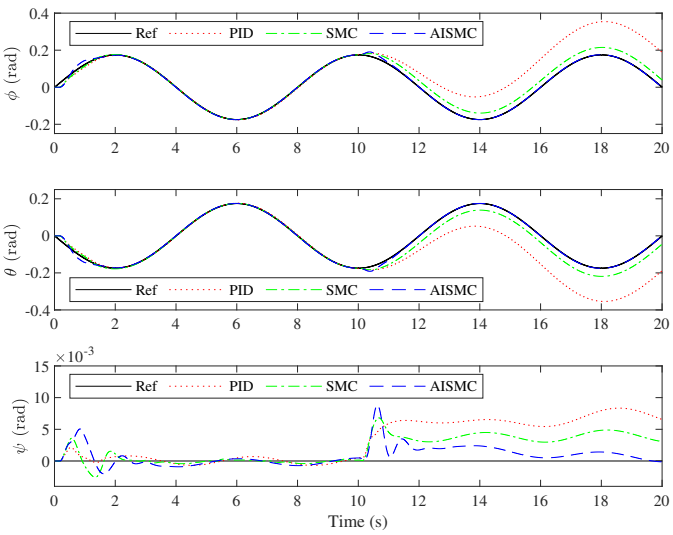

Fig. 6. Attitude responses under actuator fault.

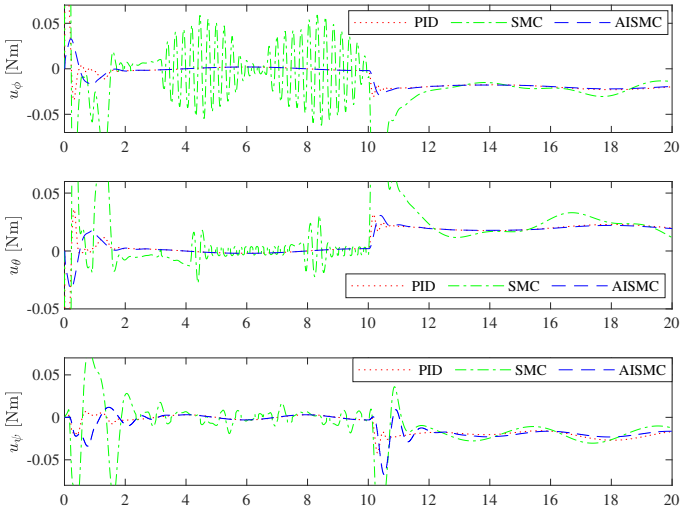

Fig. 7. Control signals under actuator fault.

gain problem in the theoretical analysis is evaluated as a fault in the actuators in the quadrotor system. Faults in the actuators are handled with adaptation laws in the controller structure, and when actuator faults occur, changes in adaptation values also occur (see Fig. 8). This result shows that the proposed control structure is not only robust against parametric and external disturbances but also against actuator faults. Moreover, no chattering is observed in the control signals across all scenarios, which is another main contribution of the proposed controller.

V. Conclusion

This technical note applies an adaptive sliding mode controller to the flight control of a quadrotor UAV, aiming to enhance robustness against external disturbances and model uncertainties. The proposed sliding mode controller is designed to be chattering-free and accounts for the bounded values of the lumped disturbances using Lyapunov-based adaptation mechanisms. The asymptotic stability of the closed-loop attitude dynamics is proven through Lyapunov's stability theory. Simulations were conducted to test the robustness

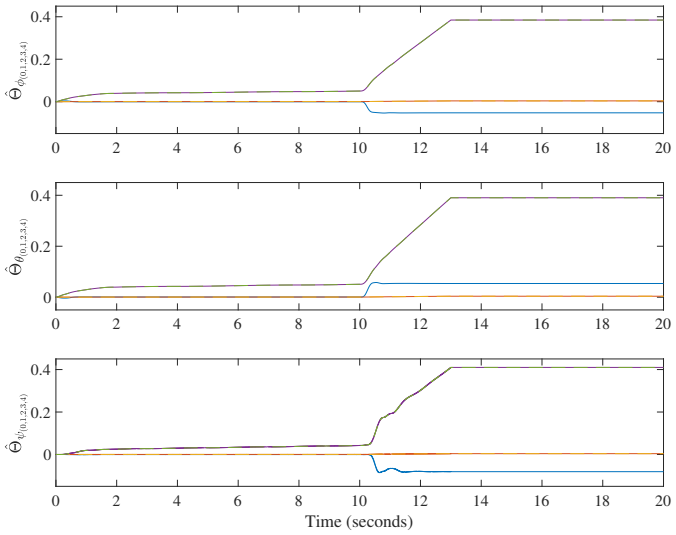

Fig. 8. Adaptations under actuator fault.

of the proposed controller against model uncertainties and external disturbances such as wind gusts. The proposed method outperforms both the PID controller and the conventional SMC by exhibiting greater robustness against external disturbances, model uncertainties, and partial actuator faults, while maintaining accurate trajectory tracking. Future work includes implementing this controller on a real-time prototype to validate the effectiveness of the proposed method.

REFERENCES

[1] H. Shraim, A. Awada, and R. Youness, "A survey on quadrotors: Configurations, modeling and identification, control, collision avoidance, fault diagnosis and tolerant control," *IEEE Aerosp. Electron. Syst. Mag.*, vol. 33, no. 7, pp. 14–33, 2018.

[2] M. Idrissi, M. Salami, and F. Annaz, "A review of quadrotor unmanned aerial vehicles: applications, architectural design and control algorithms," *J. Intell. Rob. Syst.*, vol. 104, no. 2, p. 22, 2022.

[3] H. Mo and G. Farid, "Nonlinear and adaptive intelligent control techniques for quadrotor uav–a survey," *Asian J. Control*, vol. 21, no. 2, pp. 989–1008, 2019.

[4] M. G. Patan and F. Caliskan, "Sensor fault–tolerant control of a quadrotor unmanned aerial vehicle," *Proc. Inst. Mech. Eng., Part G: J. Aerosp. Eng.*, vol. 236, no. 2, pp. 417–433, 2022.

[5] F. Adıgüzel, K. Kurtuluş, and T. Türker, "A gain scheduling attitude controller with nn supervisor for quadrotor uavs," *Int. J. Control Autom. Syst.*, vol. 22, no. 12, pp. 3777–3791, 2024.

[6] J. Kim, S. A. Gadsden, and S. A. Wilkerson, "A comprehensive survey of control strategies for autonomous quadrotors," *Can. J. Electr. Comput. Eng.*, vol. 43, no. 1, pp. 3–16, 2019.

[7] I. Lopez-Sanchez and J. Moreno-Valenzuela, "Pid control of quadrotor uavs: A survey," *Annu. Rev. Control*, vol. 56, p. 100900, 2023.

[8] S. Bouabdallah, "Design and control of quadrotors with application to autonomous flying," Ph.D. dissertation, École Polytechnique Fédérale de Lausanne, 01 2007.

[9] S. Bouabdallah, A. Noth, and R. Siegwart, "Pid vs lq control techniques applied to an indoor micro quadrotor," in *2004 IEEE/RSJ international conference on intelligent robots and systems (IROS)(IEEE Cat. No. 04CH37566)*, vol. 3. IEEE, 2004, pp. 2451–2456.

[10] Y. Yu, S. Yang, M. Wang, C. Li, and Z. Li, "High performance full attitude control of a quadrotor on so(3)," in *2015 IEEE International Conference on Robotics and Automation (ICRA)*, 2015, pp. 1698–1703.

[11] J. Yoon and J. Doh, "Optimal pid control for hovering stabilization of quadcopter using long short term memory," *Adv. Eng. Inf.*, vol. 53, p. 101679, 2022.

[12] D. Lee, H. Jin Kim, and S. Sastry, "Feedback linearization vs. adaptive sliding mode control for a quadrotor helicopter," *Int. J. Control Autom. Syst.*, vol. 7, pp. 419–428, 2009.

[13] L. Martins, C. Cardeira, and P. Oliveira, "Feedback linearization with zero dynamics stabilization for quadrotor control," *J. Intell. Rob. Syst.*, vol. 101, no. 1, p. 7, Dec 2020.

[14] J. Wang, K. A. Alattas, Y. Bouteraa, O. Mofid, and S. Mobayen, "Adaptive finite-time backstepping control tracker for quadrotor uav with model uncertainty and external disturbance," *Aerosp. Sci. Technol*, vol. 133, p. 108088, 2023.

[15] L. Guettal, A. Chelihi, R. Ajgou, and M. M. Touba, "Robust tracking control for quadrotor with unknown nonlinear dynamics using adaptive neural network based fractional-order backstepping control," *J. Franklin Inst.*, vol. 359, no. 14, pp. 7337–7364, 2022.

[16] K. Runcharoon and V. Srichatrapimuk, "Sliding mode control of quadrotor," in *2013 The International Conference on Technological Advances in Electrical, Electronics and Computer Engineering (TAEECE)*. IEEE, 2013, pp. 552–557.

[17] V. K. Tripathi, L. Behera, and N. Verma, "Design of sliding mode and backstepping controllers for a quadcopter," in *2015 39th national systems conference (NSC)*. IEEE, 2015, pp. 1–6.

[18] J. J. Castillo-Zamora, K. A. Camarillo-Gomez, G. I. Perez-Soto, and J. Rodriguez-Resendiz, "Comparison of pd, pid and sliding-mode position controllers for v–tail quadcopter stability," *Ieee Access*, vol. 6, pp. 38 086–38 096, 2018.

[19] H. Bouadi, S. S. Cunha, A. Drouin, and F. Mora-Camino, "Adaptive sliding mode control for quadrotor attitude stabilization and altitude tracking," in *2011 IEEE 12th international symposium on computational intelligence and informatics (CINTI)*. IEEE, 2011, pp. 449–455.

[20] Y. Zhang, Z. Chen, M. Sun, and X. Zhang, "Trajectory tracking control of a quadrotor uav based on sliding mode active disturbance rejection control," *Nonlinear Anal.-Model. Control*, vol. 24, no. 4, pp. 545–560, 2019.

[21] X. Shao, G. Sun, W. Yao, J. Liu, and L. Wu, "Adaptive sliding mode control for quadrotor uavs with input saturation," *IEEE/ASME Trans. Mechatron.*, vol. 27, no. 3, pp. 1498–1509, 2022.

[22] M. T. Hamayun, C. Edwards, and H. Alwi, *Integral Sliding Mode Control*. Springer International Publishing, 2016.

[23] M. Labbadi, M. Cherkaoui, Y. E. houm, and M. Guisser, "Modeling and robust integral sliding mode control for a quadrotor unmanned aerial vehicle," in *2018 6th International Renewable and Sustainable Energy Conference (IRSEC)*, 2018, pp. 1–6.

[24] S. Li, Y. Wang, J. Tan, and Y. Zheng, "Adaptive rbfnns/integral sliding mode control for a quadrotor aircraft," *Neurocomputing*, vol. 216, pp. 126–134, 2016.

[25] A. Eltayeb, M. F. Rahmat, M. A. M. Basri, and M. S. Mahmoud, "An improved design of integral sliding mode controller for chattering attenuation and trajectory tracking of the quadrotor uav," *Arabian J. Sci. Eng.*, vol. 45, pp. 6949–6961, 2020.

[26] K. Wang, C. Hua, J. Chen, and M. C. and, "Dual-loop integral sliding mode control for robust trajectory tracking of a quadrotor," *International Journal of Systems Science*, vol. 51, no. 2, pp. 203–216, 2020.

[27] S. C. Yogi, V. K. Tripathi, and L. Behera, "Adaptive integral sliding mode control using fully connected recurrent neural network for position and attitude control of quadrotor," *IEEE Trans. Neural Networks Learn. Syst.*, vol. 32, no. 12, pp. 5595–5609, 2021.

[28] A. Eltayeb, M. F. Rahmat, M. A. M. Basri, M. M. Eltoum, and M. S. Mahmoud, "Integral adaptive sliding mode control for quadcopter uav under variable payload and disturbance," *IEEE access*, vol. 10, pp. 94 754–94 764, 2022.

[29] V. K. Tripathi, A. K. Kamath, L. Behera, N. K. Verma, and S. Nahavandi, "An adaptive fast terminal sliding-mode controller with power rate proportional reaching law for quadrotor position and altitude tracking," *IEEE Trans. Syst. Man Cybern.: Syst.*, vol. 52, no. 6, pp. 3612–3625, 2021.